Journal of Geochemical Exploration 176 (2017) 33–41

Contents lists available at ScienceDirect

Journal of Geochemical Exploration

journal homepage: www.elsevier.com/locate/gexplo

Geochemical characteristics of heavy metal contamination induced by a sudden wastewater discharge from a smelter

Yongqiang Yuan [a,*], Meng Xiang [b], Congqiang Liu [a], Benny K.G. Theng [c]

[a] State Key Laboratory of Environmental Geochemistry, Institute of Geochemistry, Chinese Academy of Sciences, Guiyang 550002, China
[b] Huatian Engineering & Technology Corporation, MCC, Nanjing 243000, China
[c] Landcare Research, Private Bag 11052, Palmerston North 4442, New Zealand

A R T I C L E I N F O

Article history:
Received 13 May 2015
Revised 19 April 2016
Accepted 4 July 2016
Available online 5 July 2016

Keywords:
Wastewater overflow
Heavy metal
Contamination
Enrichment
Mobility

A B S T R A C T

Metal contaminations from smelting have been widely reported, however, the study on metal mobility or transfer characteristics in soil profiles after a sudden wastewater overflow is far limited. This study was undertaken to investigate distribution and potential mobility of heavy metals in soils flooded by smelting wastewater in Hechi, China. Total heavy metal/metalloid levels were measured in topsoil, profile and profile pore-water taken in-situ. Enrichment factor (EF) and nemero synthesis index (P_N) were used to detect the contribution of anthropogenic emissions to trace element fluxes and pollution levels, respectively. Soil-water partition coefficient (K_d) was used to reflect the fate and the mobility of elements. Results showed topsoil were seriously contaminated with Sb (289–3100 mg kg^{-1}), Pb (444–6388 mg kg^{-1}), Zn (294–923 mg kg^{-1}), Cu (59–192 mg kg^{-1}), Cd (12–34 mg kg^{-1}), and As (32–405 kg^{-1}), and P_N values indicated this area was in severe or strongly pollution level. Higher EF values of Sb, Zn, Cd and As were found in the flooded soils, and P_N in flooded area was 5 times of that in the unflooded sites, indicating wastewater flooding aggregated pollution in the low-lying area. The Sb, Pb, and Cd concentrations declined drastically with profile but dropped to constant levels below a depth of about 20 cm. In contrast, Zn and Cu in flooding soils declined first and then increased to another extreme value even at depth of 50 cm. Pore-water profiles exhibited the similar declining trends of vertical metal/metalloid distribution pattern. The K_d values ranged from 10^2–10^6 L kg^{-1}, and the mobility and bioavailability of the six elements in the profiles declined in the following order: Sb > Zn > Cu > Cd > As > Pb. The relatively low K_d values for some depth intervals may reflect adsorption decrease or migration increase of metal/metalloid. However, it is worth to further study and assess their potential risk to environment in longer period.

1. Introduction

Soil heavy metal contamination is a relevant environmental problem worldwide that increases human health risks, and ecotoxicity, due to their high persistence and large capacity of bioaccumulation (Popescu et al., 2013; Galal and Shehata, 2015). Metalliferous smelting processes are one of the most anthropogenic pollution sources and many studies about soil metallic pollution arising from smelter dry fallout/fly ash, solid waste have been carried out in the proximity of metallurgical sites (Pelfrene et al., 2011; Douay et al., 2013; Popescu et al., 2013; Guo et al., 2014; Li et al., 2015). Generally, combined contaminations of toxic heavy metals co-occurred in these sites. A research showed that significantly Sb (235.8 mg kg^{-1}), Cd (51.8 mg kg^{-1}) and Hg (13.8 mg kg^{-1}) were accumulated in soil in Xikuangshan mining area (Wang et al., 2010). Metals of Pb, Cd, Cu and Zn in soils near a smelter reached 4000, 9.9, 1191 and 1564 mg kg^{-1}, respectively (Popescu et al., 2013). Multiple soil contamination of Cd (63.5 mg kg^{-1}), Cu (198 mg kg^{-1}), Pb (3330 mg kg^{-1}) and Zn (16,300 mg kg^{-1}) was reported from a former illegal dump site in Italy (Petriccione et al., 2013). Li et al. (2015) also reported As, Cd, Cu, Pb, Sb and Zn contents in soils were as high as 29.9 12.8, 239, 712, 6.4, and 1688 mg kg^{-1} around a smelter in Huize, China. However, the mobility or transfer characteristic of heavy metals in soil influenced by sudden pollution accidence, such as wastewater overflow from a smelter, has rarely been reported.

Additionally, in polluted soil systems, water-soluble contaminants were more critical than the total contents due to their ecological and environmental impact (Beesley and Marmiroli, 2011; Pelfrene et al., 2011; Ettler, 2016). Since the dissolved heavy metals and metalloids can be transported through pore-water advection, convection and solute diffusion/dispersion, and contaminate both soil and groundwater (Zhao et al., 2007; Khalil et al., 2013). However, most of the studies had evaluated water-soluble metal fractions through selective extractions and leaching test in conjunction with laboratory based methods (Ettler

---

* Corresponding author at: State Key Laboratory of Environmental Geochemistry, Institute of Geochemistry, CAS, China.

E-mail address: huayang1202@sohu.com (Y. Yuan).

http://dx.doi.org/10.1016/j.gexplo.2016.07.005
0375-6742/

et al., 2010; Pelfrene et al., 2011; Boussen et al., 2013; Guo et al., 2014), which may disturb soil structure or destroy the soil matrix, and cannot reflect the nature of element migration in soils in-situ conditions (Beesley et al., 2010; Moreno-Jimenez et al., 2011). Recently, interstitial pore-water sampling techniques have proved to be effective, which will be better indicating element transportation in-situ (Clemente et al., 2008; Beesley et al., 2010; Shaheen et al., 2014).

Jinhai Metallurgy Chemical Industry, a lead and antimony smelter near Hechi City, Southwest China, produced wastewater with a high content of heavy metals. The smelter was started in 1992 and shut in 2008, because of a sudden overflow event of the smelting wastewater during storms. Studies have been carried out to investigate multiple metal contaminations in surrounding soils (Tserenpil and Liu, 2011; Yuan and Liu, 2011). Nevertheless, mobility and potential ecological risk of trace elements in profile affected by the accidents of emergency pollution were unknown.

The aim of this study was to investigate distribution and potential mobility of heavy metals in soils flooded by smelting wastewater after a sudden overflow accident. For this purpose, we first assess metal contamination levels in soils from both flooded and unflooded sites near the smelter. In addition, to determine the mobility or potential movement of metals and metalloids downwards, we measured the metal concentrations from profiles and pore-water taken in-situ from the soil profile.

2. Materials and methods

2.1. Study area

The study area was located near an abandoned smelter (108°03′E, 24°43′N), in the suburb of Hechi City, in northwest Guangxi, China. This area has a humid subtropical climate with mean annual temperature of 20.4 °C and a rainfall of 1470 mm. The soil is generally classified as terra fusca. The year leading wind direction is prevailing southwesterly winds. The smelter lies in a valley, 180–210 m above sea level, with two villages nearby. The main minerals in the former smelter were stibnite (Sb_2S_3), antimonite ($FeSb_2S_4$) and plaglonite ($Pb_5Sb_8S_{17}$). It was closed down in 2008, following a sudden overflow event of the smelting wastewater during storms. The sampling sites were divided into two parts by the outflow smelting wastewater, the flooding site (site A) in front of the wastewater tank and the unflooded site (site B) near the foot of the hills. The area approximately 8.4 km southwest from the smelter was chosen as control site (site C). Sketch of sampling points are seen in Fig. 1.

2.2. Sampling and sample pre-treatment

Topsoil (approximately 0–10 cm depth) samples were taken at A, B and C sites, and soil profiles (0–10 cm, 10–20 cm, 20–40 cm, 40–60 cm, 60–80 cm, 80–100 cm depths) were collected at the flooding Site A and unflooded Site B. The soil samples were transferred to acid-washed dark-colored wild-mouth bottles and transported to the laboratory. After homogenization, the soils were air-dried, slightly crushed, passed through a 2-mm sieve, and stored in glass bottles. Pore-water of the profiles at site A was collected by Rhizon soil moisture sampler (Eijkelkamp, Netherlands), filtered (0.45 μm), and acidified to $pH < 2$ with HNO_3 and transferred to 4 °C refrigerator before analysis. Smelting wastewater from the outfall was also treated as pore-water sample before analysis. Flue dusts along the chimney were collected by portable dust sampler (ZC-F).

2.3. Sample analysis, quality assurance

The pH of each soil sample was analyzed in a 1:10 soil/water suspension using a combination pH electrode (Hanna pH meter). Soil organic matter (SOM) concentrations were measured by elemental analyzer (PE2400), after fumigated by dilute HCl (6 M). Portions of the soil samples were further ground (<0.149 mm) and digested with HNO_3-HF, and the Sb, Cd, Pb, Cu, Zn and As in the extracts were determined by inductively coupled plasma mass spectrophotometry (ICP-MS, Element Germany). Dust samples were digested and tested as soils. Trace elements in water samples were also measured by ICP-MS. Heavy metal oxides Al_2O_3 (%), CaO (%), Fe_2O_3 (%) and SiO_2 (%) were directly determined by wavelength dispersive X-ray fluorescence spectrometry (XRF, Axios PW4400). The mineralogical composition of soils was measured by X-ray Diffractometer (XRD, D/max-2200/PC). The accuracy of each method was assessed by replicate analyses of the elements in the certified reference materials (GBW-07,404 for national standard soils). Blank reagent was examined to exclude laboratory contamination. The precision and bias of chemical analysis were <10%, respectively. In particular, the recoveries of the elements were in the range of 98.1–105% for Sb, 92.9–104% for As, 94.7–103% for Zn, and 93.0–102% for Cu, 93.3–102% for Cd.

2.4. Quantification of soil pollution

Smelting activities generally have important effect on the elemental contents in soils. The enrichment factor (EF) was usually used to detect the contribution of anthropogenic emissions to trace element fluxes. The formula (Eq. (1)) used to calculate EF was:

$$EF = (TM/Al)_{sample}/(TM/Al)_{reference} \tag{1}$$

where TM and Al represent trace metal and aluminum contents, respectively. Al is used as reference element, due to relatively inert with respect to chemical weathering, and it has no significant anthropogenic source (Bourennane et al., 2010). To improve the sensitivity of the EF to the smelting influence, the soil at a control site (site C) was used as a reference material.

The nemero synthesis index was quantified to evaluate the pollution risk. The indexes can be computed as follows:

$$P_N = \sqrt{\left((\max P_i)^2 + \left(1/n\sum_{i=1}^{n} P_i\right)^2\right)/2} \tag{2}$$

where, the P_N is the integrated evaluation score corresponding to each site, and $P_i = C_i/S_i$ is the single factor index. C_i is the measured content of an element at each sample point, and i denote some element, and S_i is the evaluation criterion of the ith kind of element. In this study, the evaluation criterion value refers from environmental quality standards for Chinese soils (GB15618–2008) (MEPPRC, 2008). The pollution distribution was classified into the following classification: practically unpolluted ($P_N \le 0.7$), unpolluted to moderately polluted ($0.7 < P_N \le 1.0$), moderately polluted ($1.0 < P_N \le 2.0$), moderately to strongly polluted ($2.0 < P_N \le 3.0$), severe or strongly polluted ($P_N > 3$).

The partitioning of trace metals between solid and aqueous phases is often quantified by a distribution coefficient (K_d) (Sauve et al., 2000). An estimate of the K_d value can be made by:

$$K_d = C_t/C_{pw} \tag{3}$$

where C_t and C_{pw} denote the total and pore-water metals respectively and K_d is an observed distribution coefficient.

2.5. Statistical analysis

To quantify element spatial variability of regionalized variables and provide basis of spatial interpolation, the geostatistical interpolation method like kriging was used (Saby et al., 2009). For kriging estimation, the semivariogram r(h) was used to quantify the spatial dependence of soil heavy metal concentrations (Goovaerts, 1997). Kriging interpolation and mapping were conducted using ArcGis 10.0 (ESRI Inc., USA).

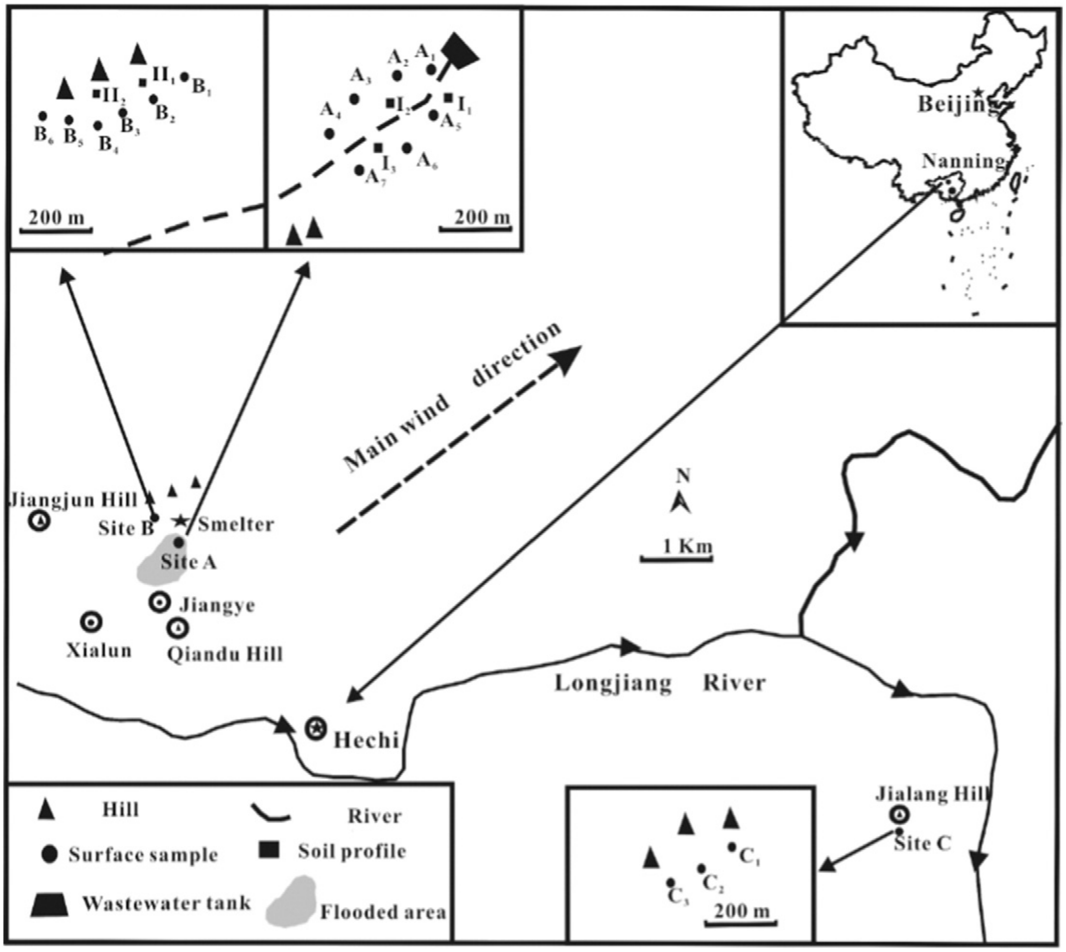

Fig. 1. Location of the study area and distribution of soil sampling points in the vicinity of a smelter in Hechi, Guangxi, China.

To quantify factors (e.g. pH, SOM and soil clay) influence the vertical distributions of trace metal/metalloid in soil profiles (Saby et al., 2009; Sen Gupta and Bhattacharyya, 2012; Rashad et al., 2014), correlation analyses and a principal component analysis (PCA) were carried. To reduce distortions and low significance of the results, a log-transformation was performed for all measured values in soil profiles (Li and Feng, 2010). All statistical data processing was carried out using the SPSS.16.0 (SPSS Inc., Chicago, IL, USA).

3. Results and discussion

3.1. Soil properties

A descriptive summary of soil properties was listed in Table 1. The soil pH in polluted sites and control site varied around 5.94 and 7.05, respectively. Soils collected from the flooding site were in lower pH values (4.88–6.54) due to the acid smelting effluent, while pH values in the unflooding soils were a little higher (5.24–6.92), but soil pH increased with depth. The SOM content ranged from 1.05% to 2.96%, and the top layer had a little higher SOM levels. Silicon dioxide (SiO_2), Al_2O_3 and Fe_2O_3 are the three most abundant compositions of soils, ranging from 76% to 81%, 10.5% to 11.0% and 4.90% to 5.18%, respectively. The concentrations of Mn and Ti varied a little larger between the smelter adjacent area (A and B sites) and the control site, ranging from 0.09% to 0.18% and 0.40% to 0.72%, respectively, whereas other soil compositions changed slightly, MgO ranged from 0.43% to 0.51%, CaO from 0.88% to 1.04%, Compared with upper crust, the studied area is rich in SiO_2 but lack of other main elements (Condie, 1993). According to XRD analysis, the proportion of mineralogical compositions of soils also changed slightly, sand (76–80%), clay (17.9–21.2%) and silt (1.02–2.75%), and there were small amounts of plagioclase (0.08–0.23%), chlorite (0.48–0.54%), and calcite (0.56–0.85%). However, a little anatase (0.07%) was detected in the polluted soils, probably due to wet-dry deposition from smelting. Similarly, the clay levels also declined slightly with soil profiles (data not shown).

Table 1
Selected chemical properties of the topsoil (mean ± standard deviation).

Site	pH (H_2O)	SOM (%)	Al_2O_3 (%)	Fe_2O_3 (%)	CaO (%)	Mn (%)	Ti (%)	MgO (%)	Clay[a] (%)	Sand (%)	Silt (%)
A (10)	5.86 ± 0.58	2.96 ± 0.30	11.0 ± 2.30	4.90 ± 0.94	1.04 ± 0.66	0.18 ± 0.02	0.72 ± 0.20	0.51 ± 0.16	21.3 ± 4.07	76 ± 7.07	2.75 ± 1.28
B (8)	6.03 ± 0.50	1.05 ± 0.42	10.5 ± 2.76	5.04 ± 1.25	0.89 ± 0.60	0.15 ± 0.04	0.69 ± 0.09	0.48 ± 0.19	19.8 ± 3.38	78 ± 4.33	2.22 ± 2.34
C (3)	7.05 ± 0.19	1.77 ± 0.16	10.7 ± 2.05	5.18 ± 0.69	0.88 ± 0.17	0.09 ± 0.03	0.40 ± 0.05	0.43 ± 0.11	17.9 ± 1.64	81 ± 3.22	1.02 ± 0.68
Upper crust[b]	–	–	14.9	4.68	3.55			2.46	–	66.3	–

[a] Average of clay minerals content: kaolinite (9.77%–11.7%), montmorillonite (4.02%–5.23%), illite (4.05%–4.88%).
[b] (Condie, 1993).

3.2. Spatial variations of trace metal/metalloid in soils

The total metal/metalloid contents in the topsoil were present in Table 2. Soils collected from the control site harbored 18–23 mg kg^{-1} of Sb, 34–45 mg kg^{-1} of As, 68–87 mg kg^{-1} of Pb, 19–31 mg kg^{-1} of Zn, 8–14 mg kg^{-1} of Cu, and 1.6–2.5 mg kg^{-1} of Cd, respectively. The contents of soil Sb, Pb, As and Cd were higher than their corresponding levels in worldwide uncontaminated soils (Khalil et al., 2013; Li et al., 2015). Meanwhile, soil Sb, As, Pb and Cd concentrations were also 2–32 folds as high as that in the "background" soil of Guangxi (Guangxi Institute of Environmental Protection, 1992). This finding is probably related to the geology of the study site. Hechi is located in the Nanling metallogenic belt. It was reported Guangxi accounted for 34.4% of Sb deposits in China, most of which were distributed in northwest part of the province (He et al., 2012). Therefore metal concentrations in control site were considered as reference or baseline values when EF was calculated. While, Zn and Cu contents in control site were lower than Guangxi, largely due to mobility or leaching of the metals.

The content of each trace element in the topsoil was extremely higher than that of the baseline values, Guangxi, China and other soils of the world (Wei et al., 1990; Kabata-Pendias, 2010). The metal/metalloid contents in flooded site A were about 3–16 times of that in unflooded site B. Therefore, there was obvious a positive correlation between the extent of heavy metal contamination to the soil compartment and effluent flooding. The most seriously contaminated metals in soil were Sb, Pb, Zn, Cd, and As, which exceeded the second grade of Environmental Quality Standards for Soil of China by 157–310, 36–80, 2.1–4.6, 50–340 and 8.5–13 times, respectively (Table 2) (GB15618–2008) (MEPPRC, 2008). The data were compared to the available information on Sb in other smelting sites. It was reported soil Sb levels were up to 5050 mg kg^{-1} around smelter in Xikuangshan area (He, 2007). Forest soils near a lead smelter were enriched in 2058 mg Sb kg^{-1} (Ettler et al., 2010), and very high levels up to 80,200 mg kg^{-1} in another old smelting site was also reported (Wilson et al., 2004).

Typically, high contents of other heavy metals co-occurred with Sb in polluted sites. Telford et al. (2009) reported high contents of As (777 mg kg^{-1}) and Sb (60 mg kg^{-1}) were present in creek rhizome sediment, and EF values also showed that significantly Sb (235.8), Cd (51.8), Hg (13.8), As (3.13), Zn (2.91), Pb (2.46), and Cr (1.67) were accumulated in soil in Xikuangshan mining area (Wang et al., 2010). Similar studies showed enrichment of heavy metals in soils near Zn smelter sites. For example, Popescu et al. (2013) reported concentrations in soils near the smelter reaching 4000, 9.9, 1191 and 1564 mg kg^{-1} for Pb, Cd, Cu and Zn respectively. Li et al. (2015) also reported As, Cd, Cu, Pb, Sb and Zn contents in soils were as high as 29.9 12.8, 239, 712, 6.4, and 1688 mg kg^{-1} around a smelter in Huize, China. In addition, multiple metal contamination was also reported from a former illegal dump site in Italy, where soil heavy metal concentrations ranged as high as 63.5, 198, 3330 and 16,300 mg kg^{-1} for Cd, Cu, Pb and Zn, respectively, after an unknown smelter spreading on soil (Petriccione et al., 2013). Therefore, levels of soil metal contamination have close relations with smelting activities.

Ordinary kriging here was used to quantify the metal spatial variability of the polluted areas (A and B sites). The spatial distribution maps of heavy metals in soils based on spatial structural analysis and their concentration were shown in Fig. 2. Spatial distributions of metal/metalloid were similar to each other showing a declining trend with distance to the smelter in unflooded sites, but obvious polluted zones (expect Cd) were observed at sites II_1 and II_2 at the foot of the hills (Fig. 2a, b, e and f), probably due to the surface soil received pollution input from hillside erosion (Atucha et al., 2013; Peng et al., 2014). In the flooded area, generally, highly polluted sites of the six elements were distributed near the wastewater tank (Fig. 2a to f), however, unlike the flooded area, metal/metalloid concentrations did not follow the decreasing routine with distance to the tank, but a radially decreasing trend along the sewage ditch and some sites (e.g. A_2 and A_3) were not in the significant polluted zone. Such results might be owing to the higher topography and shorter flooding time in these sites, especially for As and Zn (Fig. 2b and e) (Acosta et al., 2011). In addition, spatial distributions of the six elements (especially Pb and Cu) (Fig. 2c and f) highlighted significant polluted zones corresponding to the wastewater flooding.

3.3. Environment risk assessment

Based on soil environmental quality standard values: (Sb < 100 mg kg^{-1}, As < 40 mg kg^{-1}, Pb < 80 mg kg^{-1}, Cd < 0.3 mg kg^{-1}, Zn < 200 mg kg^{-1}, Cu < 50 mg kg^{-1}) (MEPPRC, 2008), the elements risk and their environmental impact according to the nemero synthesis index evaluation were shown in Fig. 3. The results revealed the single factor index of hazardous metals was higher than 1, indicating the hazardous metals/metalloid had significantly polluted the adjacent area of the smelter. For example, in flooded area, the P_i value ranged from 111 to 470 for Sb among the samples, 3.4 to 16.7 for As, 39 to 115 for Pb, 55 to 167 for Cd, 2.13 to 7.42 for Zn and 2.18 to 5.26 for Cu. Although compared with the flooded area, the single factor indexes were much lower in the unflooded sites, they also had significant higher P_i values of Sb, Pb and As than other study (Li and Feng, 2010). Meanwhile, the nemero synthesis index further elucidated the contamination level of whole hazardous elements between the flooded and unflooded sites. According to the calculated data and classification of pollution levels, both areas were strongly polluted ($P_N > 3$), and Sb was the most severe pollution factor, highlighting the smelting activities causing serious pollution to the adjacent areas (Wang et al., 2010). Additionally, P_N in the

Table 2
Basic statistical parameters of heavy metals/metalloid for the topsoil (mean ± standard deviation).

	Sb	As	Pb	Zn	Cu	Cd
Flooded (10)	3100 ± 1568	405 ± 256	6388 ± 2891	923 ± 422	192 ± 58	34 ± 15
Unflooded (8)	289 ± 165	32 ± 14	444 ± 356	294 ± 126	59 ± 38	12 ± 6
Effluent (8)	13,306 ± 6514	5211 ± 2218	935 ± 319	4806 ± 2004	584 ± 238	47 ± 59
Flue dust (9)	15,165 ± 8962	3967 ± 1564	2252 ± 1653	1033 ± 587	794 ± 356	42 ± 31
Control (3)	21	39	76	26	10	2
Guangxi[a]	2.12	20	18.8	46	21	0.062
China[b]	1.2	11.2	26	74	23	0.1
World[c]	1.0	6.0	35	90	30	0.4
EQSS[d]	10	30	80	200	50	0.3
$EF_{flooded}$	147	10.4	84	36	19	17
$EF_{unflooded}$	14	0.82	5.84	11	5.9	6

Note:
[a] Guangxi (Guangxi, 1992).
[b] China (Wei et al., 1990).
[c] World (Kabata-Pendias, 2010).
[d] EQSS (MEPPRC, 2008).

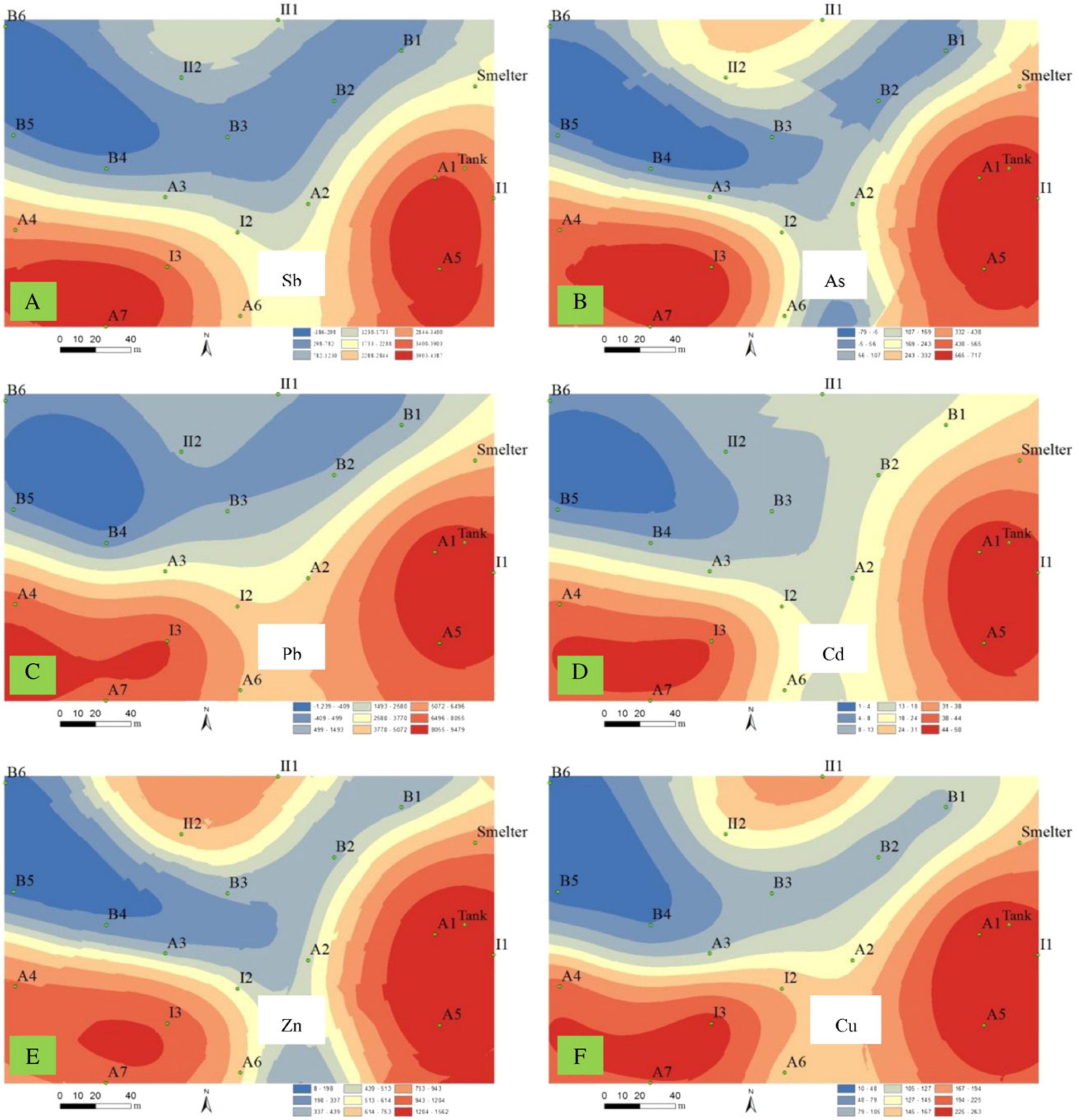

Fig. 2. Kriging maps of spatial distribution of soil heavy metals in the polluted area around the smelter.

flooded area was over 8 times of that in the unflooded area, indicating the pollution caused by the sudden pollution accident was more serious.

3.4. Vertical distributions of trace metals/metalloid in soil profiles and pore-water

In soil profiles, all the 6 elements were enriched significantly in the 0–20 cm top layer, and then declined with profile and dropped to constant levels below a depth of about 20 cm. In site A, metal contents in top layer soils were 2 times higher than that in site B (Fig. 4). The results were consistent with other studies (Bi et al., 2006; Boussen et al., 2013; Li et al., 2015). But Zn and Cu in flooding area were exception, declining first and then increasing again. Even in the depth of 50 cm in site A flooded by wastewater, soils had higher Zn and Cu contents up to 4005 and 225 mg kg^{-1}, respectively (Fig. 4a), which illustrated the mobility of Zn and Cu in our study area were stronger in acid soil. Similar results were also found for Zn in other smelter site (Bi et al., 2006; Boussen et al., 2013). The Sb, Pb, and Cd content exhibited a similarly abrupt decreasing trend at top layer, whose contents decreased drastically from 2683, 2436, and 25 mg kg^{-1} at 0–10 cm depth to 336, 289 and 14 at 10–15 cm depth, respectively. Largely due to these elements were strongly accumulated in the top 10 cm of acidic soil with high organic content (Wilson et al., 2010; Ettler et al., 2012), whereas, the reducing trend of Zn and As in site B profile were unclear, probably because of the lower contents.

Wastewater flooding also affected the profile pore-water metals/metalloid concentrations, which may reflect metal mobility or availability (Beesley et al., 2010). Similarly, metal/metalloid peak concentrations in pore-water were also present at 0–5 cm layers, where Sb, Pb, As, Zn, Cu and Cd concentrations were 1554, 63, 129, 917, 128 and 142 μg L^{-1}, respectively. The observed Sb, As, and Cd concentrations in pore-water exceeded the Class IV water quality standards of Groundwater Quality

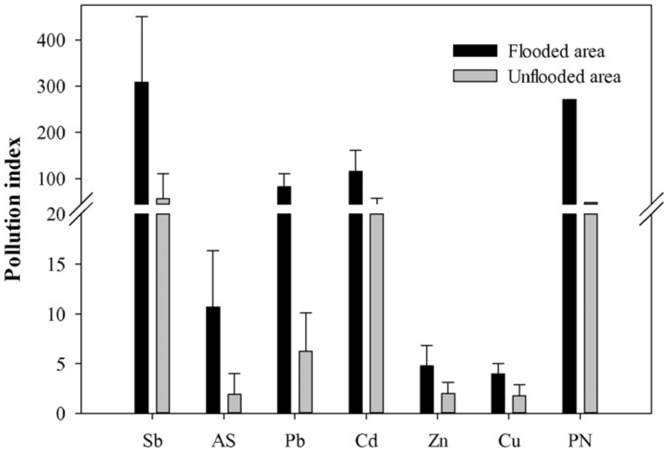

Fig. 3. Hazardous metals/metalloid and nemero synthesis index.

Standards for several depth intervals (Sb ≤ 0.05, As ≤ 0.05 and Cd ≤ 0.01 $\mathrm{mg\ L^{-1}}$) (DZ/T 0290–2015, publicity draft) (MLRPRC, 2015), thus suggesting that the flooding soil may represent a risk to benthic ground water. Metals/metalloid distribution in pore-water exhibited the similar declining trends as that in soil (Fig. 4c), dropping to constant levels at about 20 cm below ground. It indicated metals/metalloid were strongly attracted to the surface soils, probably due to soil interception, organic matter fixation and soil colloid adsorption (Sen Gupta and Bhattacharyya, 2012; Jalali and Moradi, 2013). Hence, elements were stopped rapid migrating further. Generally, the mobility and bioavailability of the six metals in the profiles declined in the following order: Sb > Zn > Cu > Cd > As > Pb. However, different element showed various characters. Pore-water Sb and Zn concentrations drastically declined at the top 15 cm layer, whereas, pore-water Pb concentration dropped to constant level at 10 cm depth. For Cu and Zn, they reached another extreme value at a depth of 20 and 25 cm, respectively. Although, the extreme values were present much shallower than soil profile and the peer study in UK (Beesley et al., 2010), it illustrated the migration trend of the elements downwards. For Sb, it exhibited two steps of declining, at depth of 0–15 cm and 20–25 cm, separately. It inferred that Sb probably was immobile by SOM/clay in the upper layer (0–15 cm). For Cd, whose concentration declined with depth, showing a different migration trend to that of a case study in UK (Beesley et al., 2010).

In moist environments, eluviation is probably the dominant natural mechanism for pollution spread from soil to underground water (Koutsopoulou et al., 2010; Carrasco and Girty, 2015). Metal concentrations in pore-water profiles illustrated metal leaching occurred mainly within the zone of residual weathering. Soil-water partition coefficient or K_d may reflect the fate and the mobility of metals, and was used as environmental risk assessment of metals for chronic exposure (Sauve et al., 2000; Degryse et al., 2009). During transportation in soils, metals/metalloid adsorption to the solid matrix (e.g. clay and OM) may result in a reduction of dissolved concentration and finally affect the overall rate of migration (Ettler et al., 2012). The K_d values for Cd, Sb, Cu, Zn, As and Pb partitioning in the present study range from 10^2–10^6 $\mathrm{L\ kg^{-1}}$ (Fig. 4d), of which Pb was the largest and Cd was the

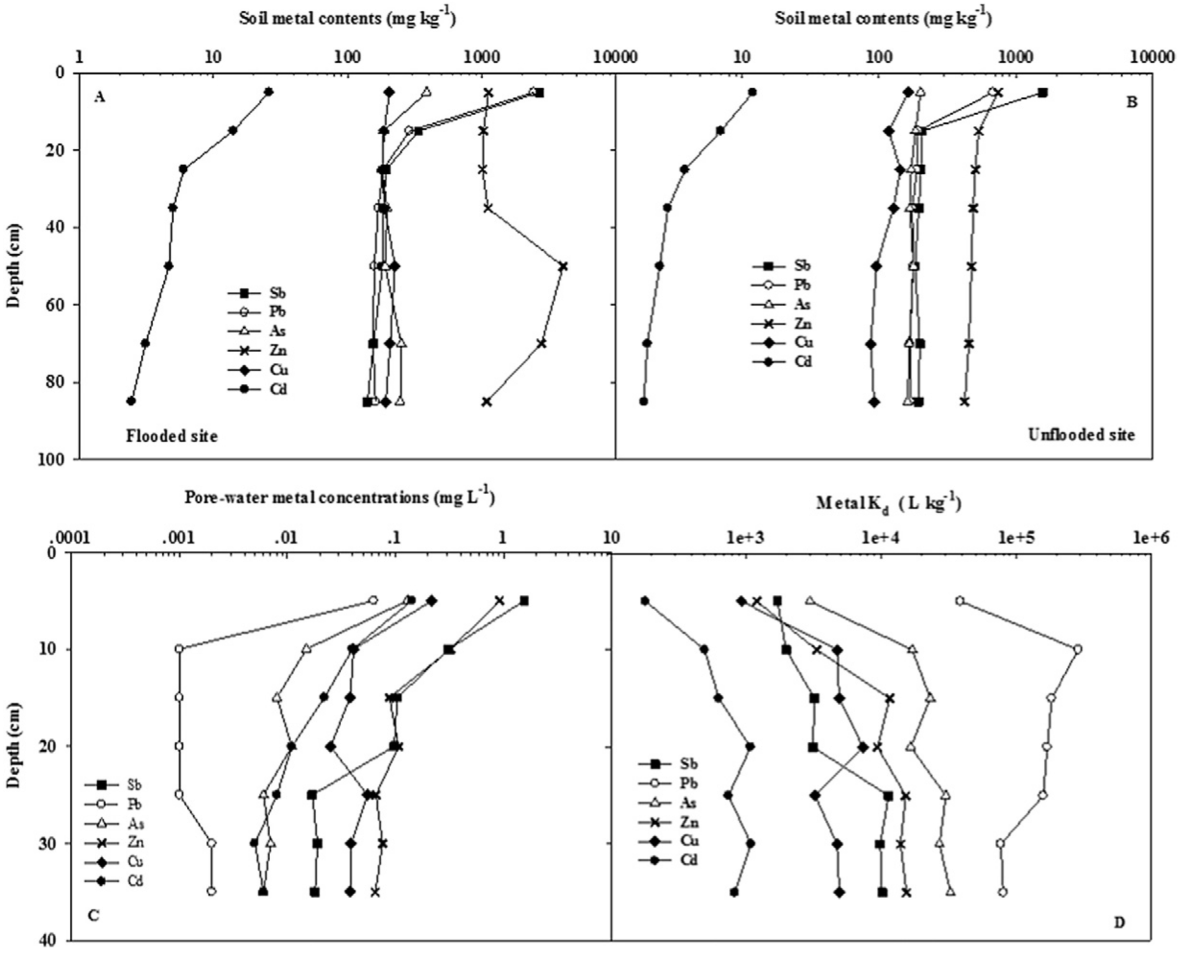

Fig. 4. Total, pore water and observed distribution co-efficient (Kd) values of Sb, As, Pb, Zn, Cu and Cd in profiles.

smallest. The relatively low K_d values for some depth intervals may reflect reduced sorption or increased migration, probably due to completed pore-water metals (Burton et al., 2005). But metal migration in short period is largely restricted by soil character such as pH, total metal burden, and organic matter and clay, and it need further study to assess their potential risk to environment.

3.5. Multivariate analysis

The mobility or leaching of element along the soil profile generally depends on the soil physiochemical properties (e.g. pH, SOM and clay), metal/metalloid properties and concentrations (Saby et al., 2009; Sen Gupta and Bhattacharyya, 2012; Rashad et al., 2014). The Pearson correlation coefficients revealed their interrelationships in soil profiles based on a log-transformation (Table 3). Results showed soil pH in the unflooded profiles exhibited high-negative significant ($p < 0.01$) correlations with the six elements, whereas SOM and clay displayed a high-positive significant correlations. It implied that SOM and clay might be the main factors influence the six elements migration downwards in the unflooded areas. In contrast, pH expressed positive or low negative correlation with Zn (0.472) or Cu (−0.238) in the flooded areas, while Sb (−0.981), Pb (−0.955), As (−0.762) and Cd (−0.942) showed strongly negative correlation scores with pH. The soil SOM indicated fairly positive relationship with Sb (0.833), Pb (0.788), and Cd (0.914), and low positive with As (0.448). In contrast, low positive or negative relationship was observed between SOM and Cu (0.031) or Zn (−0.568). The soil clay illustrated similar relationships with element concentrations in profile as SOM, as which was usually adsorbed on clays (Sen Gupta and Bhattacharyya, 2012). Therefore, that was probably the reason why Zn and Cu were easily to leach in the acidic flooded areas, as the pH value is usually an important parameter controlling the leaching of metals and metalloids (Schuwirth et al., 2007; Rashad et al., 2014).

The PCA analysis extracted using varimax rotation scheme were seen in Fig.5. The first regionalized factor, accounting for 69.9% of the total variables observed, was strongly and positively correlated with Sb, Cd, Pb, SOM and clay in the flooded areas (Fig. 5a). The variability of Zn and pH, associated with the second factor (accounting for 22.5% of the total variables), suggested high positive correlations. In addition, Cu and As were in low positively correlated with Sb, Cd, Pb, SOM and clay. In contrast, the first regionalized factor accounted for 90.7% of the total variables, and the six elements and SOM and Clay (expect pH) were strongly and positively correlated with each other in the unflooded areas (Fig. 5b). The factor analysis showed good agreement with Pearson's correlation analysis. It can be assumed that pH influence in the Zn distribution, next Cu, in profile was apparent. In contrast, metals/metalloid migrations were mainly influenced by SOM or clay in the unflooed area (Sen Gupta and Bhattacharyya, 2012; Jalali and Moradi, 2013).

4. Conclusions

Significant contamination of Sb, Pb, Cd, Zn, Cu and As was present in soil around the abandoned smelter. Nemero synthesis index indicated this area was in severe or strongly pollution level. Metals/metalloid were mainly enriched in the top layers (0–20 cm depth), and EF values were several times higher in site A than site B, indicating pollution aggravated due to the sudden wastewater overflow. The Sb, Pb, and Cd content exhibited drastically declining with profile but dropped to constant levels below a depth of about 20 cm, whereas, Zn and Cu in flooding area declined first and then increased again and reached another extreme value even at depth of 50 cm. Pore-water profiles exhibited the similar declining trends of vertical metal distribution pattern as soil, and Sb, As, and Cd concentrations in pore-water exceeded the Class IV water quality standards of Groundwater Quality Standards for several depth intervals, suggesting that the flooding soil may represent a risk to benthic ground water. Soil-water partition coefficient or K_d reflected the fate and the mobility of metals. Generally, the mobility and bioavailability of the six metals in the profiles declined in the following order: Sb > Zn > Cu > Cd > As > Pb. But Cu and Zn were easier to migrate to deeper layer in short period in acid soil, while, Sb and other metals were strongly accumulated in the top 10 cm of acidic soil with high organic content and clay. However, the mobility or leaching of heavy metals along the soil profile generally depends on the soil physiochemical properties and the metal properties and concentrations, and their potential risk to environment for long-term should be assessed in the future.

Acknowledgements

This research is supported by the Knowledge Innovation Project of the Chinese Academy of Sciences (09CJ015000) and the Innovation

Table 3
Correlation coefficients among the analyzed chemical properties (log-transformed) in soil profile.

		Sb	Pb	As	Zn	Cu	Cd	pH	SOM	Clay
Flooded area	Sb	1.000	0.986^{**}	0.769^{**}	−0.412	0.304	0.955^{**}	-0.981^{**}	0.833^{**}	0.843^{**}
	Pb		1.000	0.806^{**}	−0.356	0.342	0.933^{**}	-0.955^{**}	0.788^{**}	0.786^{**}
	As			1.000	−0.038	0.525^{*}	0.604^{**}	-0.762^{**}	0.448^{*}	0.436^{*}
	Zn				1.000	0.671^{**}	-0.490^{*}	0.472^{*}	-0.568^{**}	-0.733^{**}
	Cu					1.000	0.192	−0.238	0.031	−0.109
	Cd						1.000	-0.942^{**}	0.914^{**}	0.910^{**}
	pH							1.000	-0.869^{**}	-0.873^{**}
	SOM								1.000	0.908^{**}
	Clay									1.000
Unflooded area	Sb	1.000	0.997^{**}	0.949^{**}	0.939^{**}	0.656^{*}	0.831^{**}	-0.935^{**}	0.816^{**}	0.640^{*}
	Pb		1.000	0.954^{**}	0.944^{**}	0.674^{**}	0.827^{**}	-0.923^{**}	0.814^{**}	0.634^{*}
	As			1.000	0.975^{**}	0.738^{**}	0.922^{**}	-0.941^{**}	0.921^{**}	0.771^{**}
	Zn				1.000	0.815^{**}	0.938^{**}	-0.947^{**}	0.904^{**}	0.814^{**}
	Cu					1.000	0.778^{**}	-0.681^{**}	0.736^{**}	0.757^{**}
	Cd						1.000	-0.945^{**}	0.970^{**}	0.929^{**}
	pH							1.000	-0.906^{**}	-0.823^{**}
	SOM								1.000	0.874^{**}
	Clay									1.000

Note:
** Coefficient is significant at the 0.01 level.
* Coefficient is significant at the 0.05 level (2-tailed).

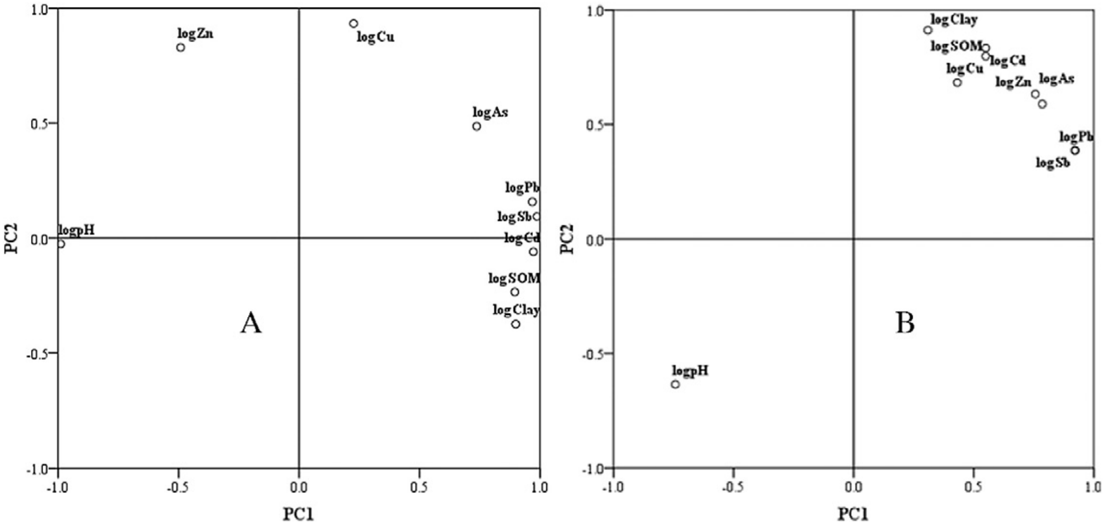

Fig. 5. Matrix of principle component analysis loadings of soil properties in profiles.

Research Group Project of the National Foundation (41021062). We gratefully acknowledge the assistance of associate professor Dong Zhang (Henan Polytechnic University) in manuscript revision and Assistant engineer Jin Guan (Institute of Geochemistry, CAS) with laboratory measurements. The authors are grateful to the anonymous reviewers whose critical comments have greatly improved the manuscript.

References

Acosta, J.A., Faz, A., Martinez-Martinez, S., Zornoza, R., Carmona, D.M., Kabas, S., 2011. Multivariate statistical and GIS-based approach to evaluate heavy metals behavior in mine sites for future reclamation. J. Geochem. Explor. 109 (1–3), 8–17.

Atucha, A., Merwin, I.A., Brown, M.G., Gardiazabal, F., Mena, F., Adriazola, C., Lehmann, J., 2013. Soil erosion, runoff and nutrient losses in an avocado (*Persea americana* Mill) hillside orchard under different groundcover management systems. Plant Soil 368 (1–2), 393–406.

Beesley, L., Marmiroli, M., 2011. The immobilisation and retention of soluble arsenic, cadmium and zinc by biochar. Environ. Pollut. 159 (2), 474–480.

Beesley, L., Moreno-Jimenez, E., Clemente, R., Lepp, N., Dickinson, N., 2010. Mobility of arsenic, cadmium and zinc in a multi-element contaminated soil profile assessed by in-situ soil pore water sampling, column leaching and sequential extraction. Environ. Pollut. 158 (1), 155–160.

Bi, X.Y., Feng, X.B., Yang, Y.G., Qiu, G.L., Li, G.H., Li, F.L., Liu, T.Z., Fu, Z.Y., Jin, Z.S., 2006. Environmental contamination of heavy metals from zinc smelting areas in Hezhang County, western Guizhou, China. Environ. Int. 32 (7), 883–890.

Bourennane, H., Douay, F., Sterckeman, T., Villanneau, E., Ciesielski, H., King, D., Baize, D., 2010. Mapping of anthropogenic trace elements inputs in agricultural topsoil from Northern France using enrichment factors. Geoderma 157 (3-4), 165–174.

Boussen, S., Soubrand, M., Bril, H., Ouerfelli, K., Abdeljaouad, S., 2013. Transfer of lead, zinc and cadmium from mine tailings to wheat (*Triticum aestivum*) in carbonated Mediterranean (northern Tunisia) soils. Geoderma 192 (1), 227–236.

Burton, E.D., Phillips, I.R., Hawker, D.W., 2005. Geochemical partitioning of copper, lead, and zinc in benthic, estuarine sediment profiles. J. Environ. Qual. 34 (1), 263–273.

Carrasco, T.L., Girty, G.H., 2015. Identifying a reference frame for calculating mass change during weathering: a review and case study utilizing the C# program assessing element immobility and critical ratio methodology. Catena 125, 146–161.

Clemente, R., Dickinson, N.M., Lepp, N.W., 2008. Mobility of metals and metalloids in a multi-element contaminated soil 20 years after cessation of the pollution source activity. Environ. Pollut. 155 (2), 254–261.

Condie, K.C., 1993. Chemical-composition and evolution of the upper continental-crust — contrasting results from surface samples and shales. Chem. Geol. 104 (1–4), 1–37.

Degryse, F., Smolders, E., Parker, D.R., 2009. Partitioning of metals (Cd, Co, Cu, Ni, Pb, Zn) in soils: concepts, methodologies, prediction and applications — a review. Eur. J. Soil Sci. 60 (4), 590–612.

Douay, F., Pelfrêne, A., Planque, J., Fourrier, H., Richard, A., Roussel, H., Girondelot, B., 2013. Assessment of potential health risk for inhabitants living near a former lead smelter. Part 1: metal concentrations in soils, agricultural crops, and homegrown vegetables. Environ. Monit. Assess. 185 (5), 3665–3680.

Ettler, V., Mihaljevic, M., Sebek, O., Valigurova, R., Klementova, M., 2012. Differences in antimony and arsenic releases from lead smelter fly ash in soils. Chem. Der Erde-Geochem. 72 (S4), 15–22.

Ettler, V., Tejnecky, V., Mihaljevic, M., Sebek, O., Zuna, M., Vanek, A., 2010. Antimony mobility in lead smelter-polluted soils. Geoderma 155 (3–4), 409–418.

Ettler, V., 2016. Soil contamination near non-ferrous metal smelters: A review. Appl. Geochem. 64, 56–74.

Galal, T.M., Shehata, H.S., 2015. Bioaccumulation and translocation of heavy metals by *Plantago major* L. grown in contaminated soils under the effect of traffic pollution. Ecol. Indic. 48, 244–251.

Goovaerts, P., 1997. Geostatistics for Natural Resources Evaluation, Oxford University Press. USA, New York.

Guangxi, Institute of Environmental Protection, 1992. Atlas of Guangxi Zhuang Autonomous Region of Soil Environmental Background Values. Chendu Cartographic Press, Chendu, pp. 122–123.

Guo, X.J., Wang, K.P., He, M.C., Liu, Z.W., Yang, H.L., Li, S.S., 2014. Antimony smelting process generating solid wastes and dust: characterization and leaching behaviors. J. Environ. Sci.-China 26 (7), 1549–1556.

He, M.C., 2007. Distribution and phytoavailability of antimony at an antimony mining and smelting area, Hunan, China. Environ. Geochem. Health 29 (3), 209–219.

He, M.C., Wang, X.Q., Wu, F.C., Fu, Z.Y., 2012. Antimony pollution in China. Sci. Total Environ. 421, 41–50.

Jalali, M., Moradi, F., 2013. Competitive sorption of Cd, Cu, Mn, Ni, Pb and Zn in polluted and unpolluted calcareous soils. Environ. Monit. Assess. 185 (11), 8831–8846.

Kabata-Pendias, A., 2010. Trace Elements in Soils and Plants. CRC press, Florida.

Khalil, A., Hanich, L., Bannari, A., Zouhri, L., Pourret, O., Hakkou, R., 2013. Assessment of soil contamination around an abandoned mine in a semi-arid environment using geochemistry and geostatistics: pre-work of geochemical process modeling with numerical models. J. Geochem. Explor. 125, 117–129.

Koutsopoulou, E., Papoulis, D., Tsolis-Katagas, P., Kornaros, M., 2010. Clay minerals used in sanitary landfills for the retention of organic and inorganic pollutants. Appl. Clay Sci. 49 (4), 372–382.

Li, P.Z., Lin, C.Y., Cheng, H.G., Duan, X.L., Lei, K., 2015. Contamination and health risks of soil heavy metals around a lead/zinc smelter in southwestern China. Ecotoxicol. Environ. Saf. 113, 391–399.

Li, X.P., Feng, L.N., 2010. Spatial distribution of hazardous elements in urban topsoils surrounding Xi'an industrial areas, (NW, China): controlling factors and contamination assessments. J. Hazard. Mater. 174 (1–3), 662–669.

MEPPRC, 2008. Environmental Quality Standard for Soils (GB15618–2008). Ministry of environmental protection of the people's Republic of China (MEPPRC), Beijing, China (in Chinese).

MLRPRC, 2015. Standard for Groundwater Quality (DZ/T 0290-2015). Ministry of Land and Resources of the People's Republic of China (MLRPRC), Beijing (in Chinese).

Moreno-Jimenez, E., Beesley, L., Lepp, N.W., Dickinson, N.M., Hartley, W., Clemente, R., 2011. Field sampling of soil pore water to evaluate trace element mobility and associated environmental risk. Environ. Pollut. 159 (10), 3078–3085.

Pelfrene, A., Waterlot, C., Mazzuca, M., Nisse, C., Bidar, G., Douay, F., 2011. Assessing Cd, Pb, Zn human bioaccessibility in smelter-contaminated agricultural topsoils (northern France). Environ. Geochem. Health 33 (5), 477–493.

Peng, X.D., Shi, D.M., Jiang, D., Wang, S.S., Li, Y.X., 2014. Runoff erosion process on different underlying surfaces from disturbed soils in the Three Gorges Reservoir area, China. Catena 123, 215–224.

Petriccione, M., Di Patre, D., Ferrante, P., Papa, S., Bartoli, G., Fioretto, A., Scortichini, M., 2013. Effects of *Pseudomonas fluorescens* seed bioinoculation on heavy metal accumulation for *Mirabilis jalapa* phytoextraction in smelter-contaminated soil. Water Air Soil Pollut. 224 (8).

Popescu, I., Biasioli, M., Ajmone-Marsan, F., Stanescu, R., 2013. Lability of potentially toxic elements in soils affected by smelting activities. Chemosphere 90 (2), 820–826.

Rashad, M., Elnaggar, E., Assaad, F.F., 2014. Readily dispersible clay and its role in the mobility of transition metals Cd^{2+}, Cu^{2+} and Zn^{2+} in an alkaline alluvial soil. Environ. Earth Sci. 71 (9), 3855–3864.

Saby, N.P.A., Thioulouse, J., Jolivet, C.C., Ratie, C., Boulonne, L., Bispo, A., Arrouays, D., 2009. Multivariate analysis of the spatial patterns of 8 trace elements using the French soil monitoring network data. Sci. Total Environ. 407 (21), 5644–5652.

Sauve, S., Hendershot, W., Allen, H.E., 2000. Solid-solution partitioning of metals in contaminated soils: dependence on pH, total metal burden, and organic matter. Environ. Sci. Technol. 34 (7), 1125–1131.

Schuwirth, N., Voegelin, A., Kretzschmar, R., Hofmann, T., 2007. Vertical distribution and speciation of trace metals in weathering flotation residues of a zinc/lead sulfide mine. J. Environ. Qual. 36 (1), 61–69.

Sen Gupta, S., Bhattacharyya, K.G., 2012. Adsorption of heavy metals on kaolinite and montmorillonite: a review. Phys. Chem. Chem. Phys. 14 (19), 6698–6723.

Shaheen, S.M., Rinklebe, J., Rupp, H., Meissner, R., 2014. Temporal dynamics of pore water concentrations of Cd, Co, Cu, Ni, and Zn and their controlling factors in a contaminated floodplain soil assessed by undisturbed groundwater lysimeters. Environ. Pollut. 191, 223–231.

Telford, K., Maher, W., Krikowa, F., Foster, S., Ellwood, M.J., Ellwood, M.J., Ashley, P.M., Lockwood, P.V., Wilson, S.C., 2009. Bioaccumulation of antimony and arsenic in a highly contaminated stream adjacent to the Hillgrove Mine, NSW, Australia. Environ. Chem. 6 (2), 133–143.

Tserenpil, S., Liu, C.Q., 2011. Study of antimony(III) binding to soil humic acid from an antimony smelting site. Microchem. J. 98 (1), 15–20.

Wang, X.Q., He, M.C., Xie, J., Xi, J.H., Lu, X.F., 2010. Heavy metal pollution of the world largest antimony mine-affected agricultural soils in Hunan province (China). J. Soils Sediments 10 (5), 827–837.

Wei, F.S., Chen, J.S., Wu, Y.Y., Zheng, C.J., Jiang, D.Z., 1990. Background Contents of Elements in China Soils. Publishing House of Chinese Environmental Sciences, Beijing.

Wilson, N.J., Craw, D., Hunter, K., 2004. Antimony distribution and environmental mobility at an historic antimony smelter site, New Zealand. Environ. Pollut. 129 (2), 257–266.

Wilson, S.C., Lockwood, P.V., Ashley, P.M., Tighe, M., 2010. The chemistry and behaviour of antimony in the soil environment with comparisons to arsenic: a critical review. Environ. Pollut. 158 (5), 1169–1181.

Yuan, Y.Q., Liu, C.Q., 2011. Pollution of agricultural soils by a wastewater outflow from a metal smelter in Guangxi Zhuang autonomous region. Environ. Sci. 32 (11), 3312–3317 (in Chinese).

Zhao, C.B., Hobbs, B.E., Ord, A., Hornby, P., Peng, S.L., Liu, L.M., 2007. Mineral precipitation associated with vertical fault zones: the interaction of solute advection, diffusion and chemical kinetics. Geofluids 7 (1), 3–18.